Mosaicing with High Dynamic Range

ROBERT BRAUN

National Radio Astronomy Observatory,[a] Socorro, New Mexico 87801

INTRODUCTION

This memo is one in a series investigating the applications and limitations of mosaicing, the imaging of objects large with respect to an interferometer primary beam using multiple pointings. In this case we consider some of the limitations to the final dynamic range and methods of circumventing these limitations. The discussion is based on the attempt to adequately reduce the observations described below.

OBSERVATIONS

A compact three pointing mosaic centered on the east central limb of the Cygnus Loop supernova remnant was observed on 5 May 1987. The observations were done in the D configuration at 6 cm, with an equilateral triangle of pointings having 7 arcmin leg length. This corresponds to a spacing of roughly 70 % of the 6 cm FWHM resulting in a slight undersampling of the primary beam. 12 hours of observing time was used to cycle 20 times through the three pointing centers. After calibration and move time overhead, slightly more than 3 hours integration time was achieved per pointing.

DATA REDUCTION

The data were edited and calibrated in the usual fashion. Initial images revealed a compact double (70 mJy, 30 mJy) background source situated within the triangle of pointings at roughly 3, 5 and 7 arcmin radius with respect to the pointing centers. Attempts to deconvolve the individual pointings with the AIPS task APCLN showed limitations in the standard calibration. The calibration was improved through one pass of phase-only self calibration for the field furthest removed from the compact double and two passes for the other two fields. This allowed deconvolution by CLEAN'ing to the 80 μJy rms level (still about twice the noise in Stoke's parameter V images made from the same data) corresponding to a dynamic range of about 1000:1.

At this point the data processing diverged into a number of different paths.

A. THE DIRECT APPROACH

In the first instance it was attempted to simultaneously deconvolve the three pointings directly. The dirty images made with the uniformly weighted self-calibrated data were interpolated unto a commom tangent plane projection and grid using a biquintic interpolating function within the AIPS task HGEOM, pre-convolved with a 15 arcsec circular Gaussian and then simultaneously deconvolved with the AIPS task

[a] The National Radio Astronomy Observatory (NRAO) is operated by Associated Universities, Inc., under contract with the National Science Foundation.

VTESS. The deconvolution could not achieve an rms fit better than about 1 mJy and although the extended emission had to some extent been reconstructed, the resulting image suffered serious artifacts in the vicinity of and radiating from the compact double. Since MEM-like algorithms are known to have difficulty in deconvolving compact features near extended emission, this may explain part of the problem. However, this limitation does not usually set in (with good u,v sampling as is the case here) before the 1000:1 level, rather than the current < 100:1. On the other hand, apparent inconsistencies amongst the pointings due to incomplete knowledge of the primary beam as well as pointing errors could easily occur at the few % level. This is because the VLA primary beam model although based on a fit to the holographic measurements of Napier and Rots (1982) is truncated at the 7 % level, beyond which lies a null and a system of non-axisymmetric sidelobes, while a pointing accuracy of 10 to 15 arcsec translates in a 10 % amplitude change at the half power point of the 6 cm beam. Another potential explanation for the unsatisfactory deconvolution may lie in the errors introduced by interpolation of the dirty images to a common grid before deconvolution. This effect has been investigated further in another case (a 10 pointing mosaic at 20 cm of M31) where it was found that a biquintic interpolation of a reasonably sampled image (2.5 points per beam) was directly responsible for a 200:1 limitation on dynamic range after deconvolution. This limitation could be avoided (if "w" term errors do not begin to dominate) by a full 3-D phase rotation of the visibility data to a common tangent plane with the AIPS task UVFIX before imaging and deconvolution. It appears likely that in view of the smaller magnitude of the other effects it is indeed pointing and/or apparent primary beam inconsistencies which are currently limiting the dynamic range in this case, although it is still conceivable that interpolation errors are to blame. To further test this hypothesis, we intend to repeat the above processing with the 3-D phase rotation to circumvent the interpolation step in the near future.

B. Initial Source Subtraction

To overcome the problems induced by the compact double, two point components determined from model fits to CLEAN'ed images were subtracted with the AIPS task UVSUB from each of the three self-calibrated u,v databases. Subsequent dirty images were then interpolated, pre-convolved and simultaneously deconvolved as before. The deconvolution via VTESS converged satisfactorily to a 70 μJy rms level, and is shown in Figure 1a. This method, although cumbersome, was quite successful in reconstructing the extended emission of interest with $\sim$ 1000:1 effective dynamic range.

C. Hybrid Approach

Since the previously described method requires both individual and joint deconvolutions of the various pointings as well as manual source fitting and subtraction it does not seem appealing as a general solution to this problem. At this point it is worth considering what it is one wishes to accomplish through mosaicing.

- Reconstruction of the largest possible structures.
- Obtaining the best possible overall reconstruction.
- Obtaining uniform sensitivity over a specified region.

All of these objectives require fully sampling the interferometer primary beam, however the first is more sensitive than the second two to the requirement of a joint deconvolution. Extracting visibility information for baselines less than a dish diameter can be accomplished with nonlinear processing in cases where the u,v sampling of each pointing is not complete. (In the case of relatively complete sampling near the origin this extraction can be done directly.) For the extraction to be effective in the current, incomplete case, it must take place during the deconvolution where the original data and associated errors are still known. The second objective is less sensitive to this requirement. Although it is still true that the effect of simultaneous deconvolution is to provide spatial frequency constraints on a broad track (corresponding to the Fourier transform of the primary beam) rather than a set of delta functions, the track width becomes a less significant fraction of the track spacing for long spacings. The goal of uniform sensitivity on the other hand can be easily satisfied by a linear combination of individually deconvolved pointings.

Since a joint deconvolution is most crucial to reconstructing the short spacings, while the goals of uniform sensitivity and longer spatial frequency reconstruction are reasonably well satisfied by individual deconvolution, it was thought appropriate to address the problem in a dual fashion. The short spacings were reconstructed by a joint deconvolution of the pointings with the AIPS task VTESS at a sufficiently low resolution that the extended source of interest dominated the field. The long spacings were reconstructed by individually deconvolving the pointings with the AIPS task APCLN. The high resolution images were then interpolated onto a common grid with HGEOM and combined with appropriate primary beam correction and weighting through a painful series of processing steps with the AIPS tasks PBCOR and COMB. The low resolution mosaic was interpolated unto this final grid and both the low and high resolution images were Fourier transformed. The amplitude near the origin of the transform plane was constructed for each and compared. As expected, the inner part of the transform plane had higher amplitude and more continuous structure in the low resolution VTESS mosaic, there was an annulus in which the two transform planes agreed and the outer part of the transform plane was only present in the high resolution linear mosaic. These two databases were merged by extracting the inner u,v plane from the VTESS mosaic and the outer u,v plane from the linear mosaic and inverse transforming the combination. The resulting image is shown in Figure 1b. and is virtually identical to the source subtracted VTESS mosaic of Figure 1a. excepting, of course, the missing background double and MEM noise suppression. This method has thus allowed the fairly automatic reduction of a mosaiced field with the dynamic range being limited only by what is achievable on the individual pointings, where all the usual methods for enhancement can be exploited. There may well be pathological cases which require some further refinement of technique. For example, if the field is dominated by the bright complex structure of the source of interest, the individual pointings could be boot-strapped with the short spacings of a low resolution mosaic to aid in their deconvolution. This approach has a further advantage in that one need never carry out the joint deconvolution at full resolution, where the problem could become unmanagable with current software. (Consider a B+C+D configuration, 10 pointing mosaic of M31 at 20 cm requiring 10 image,beam pairs of 8192 by 4096

pixels.) This is because the current VTESS requires full, mosaic-size image,beam pairs upon which full size transforms and data comparisons are carried out, even though each pointing may relate to only a small part of the total mosaic. Although this algorithmic limitation may change on a relatively short time scale the dynamic range problems are likely to remain.

The method outlined above of producing a linear mosaic has now been streamlined with the new AIPS task LTESS, while the merging of different u,v planes is now possible with the new AIPS task IMERG.

Summary

Limitations in the dynamic range of mosaiced images due to apparent inconsistencies amongst the various pointings and/or errors in the interpolation to a common grid have been considered here, as well as two techniques for overcoming them. Removal of compact confusing sources directly from the visibilities is an effective and practical method in cases where a small number of truly compact sources are at fault. A more general solution involves splitting the reconstruction problem into two segments. A low resolution joint deconvolution to reconstruct the short spacings as accurately as possible and a series of individual full resolution deconvolutions which are then combined in a linear mosaic to represent the long spacing data as well as possible. Short spacings from the former are then merged with long spacings from the latter for the final reconstruction.

References

Napier, P.J. and Rots, A.H. (1982), *NRAO test memo 134*.

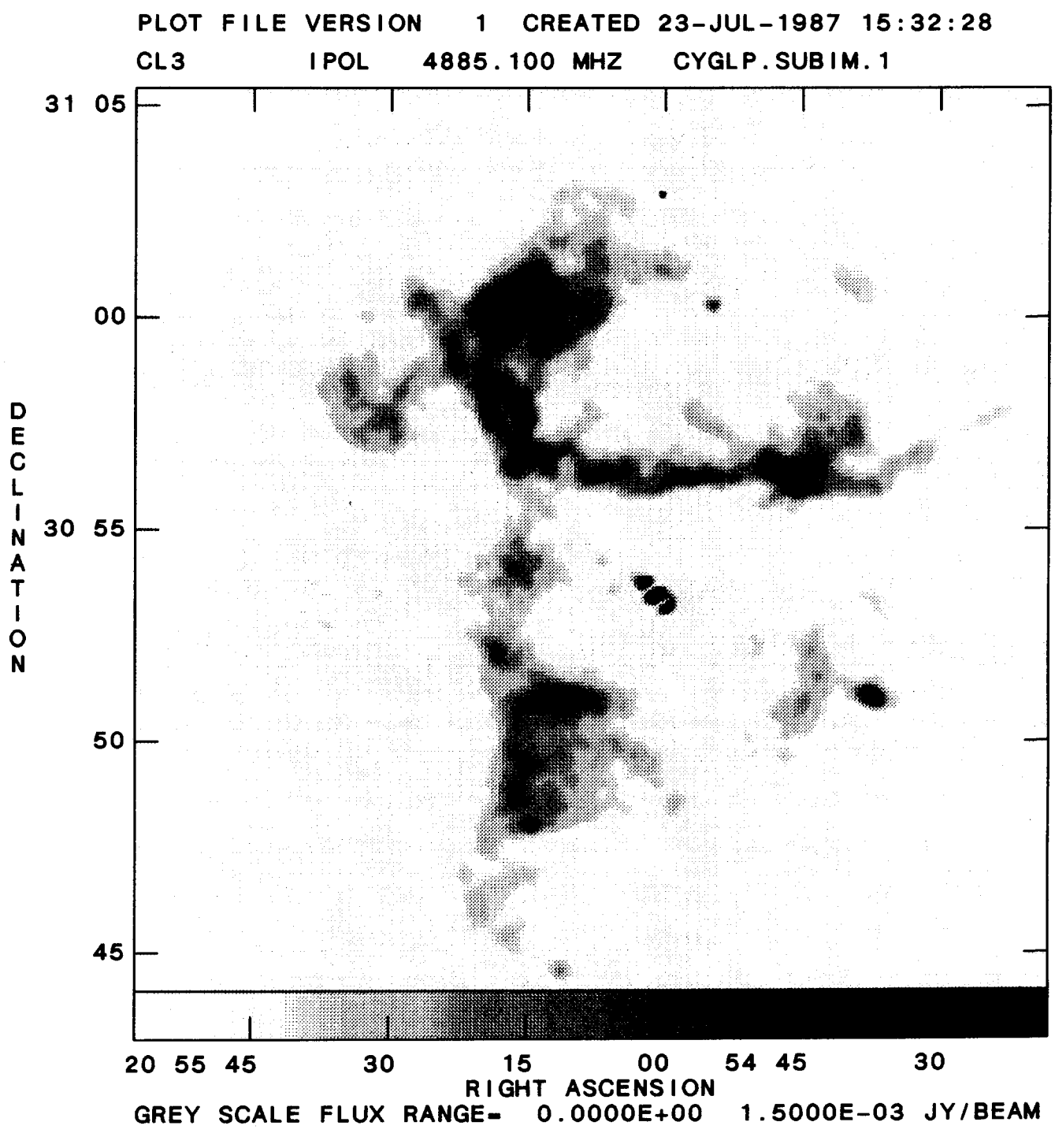
PLOT FILE VERSION 1 CREATED 23-JUL-1987 15:32:28
CL3 IPOL 4885.100 MHZ CYGLP.SUBIM.1
31 05
00
30 55
50
45
DECLINATION
20 55 45
30
15
00
54 45
30
RIGHT ASCENSION
GREY SCALE FLUX RANGE= 0.0000E+00 1.5000E-03 JY/BEAM

Figure 1a.

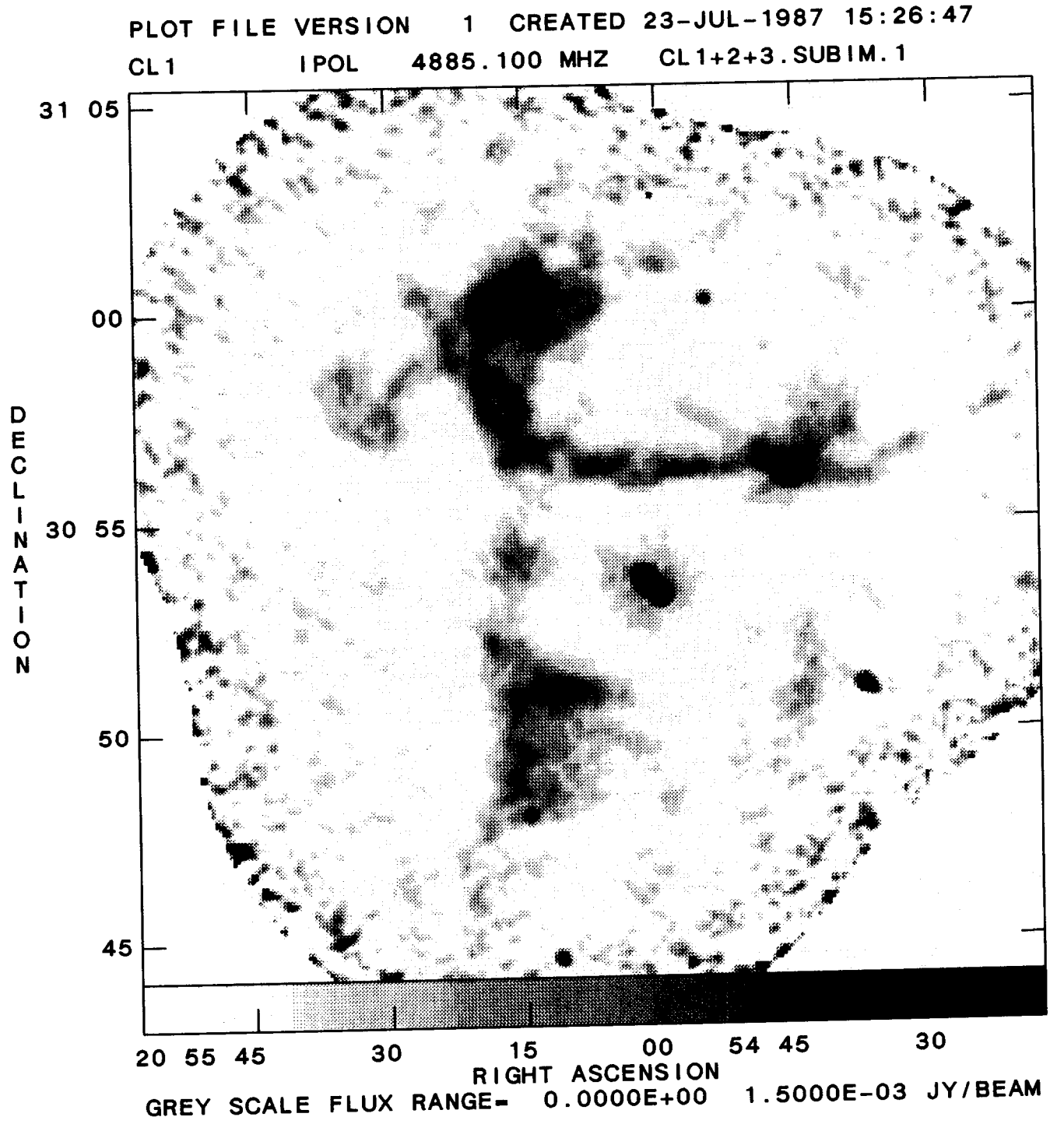
PLOT FILE VERSION 1 CREATED 23-JUL-1987 15:26:47
CL1 IPOL 4885.100 MHZ CL1+2+3.SUBIM.1
31 05
00
30 55
50
45
DECLINATION
20 55 45
30
15
00
54 45
30
RIGHT ASCENSION
GREY SCALE FLUX RANGE= 0.0000E+00 1.5000E-03 JY/BEAM

Figure 1b